

Precise theoretical prediction on branching fractions and polarizations of $D \rightarrow VV$ decays

Jing Ou-Yang¹, Hui Zheng¹, Run-Hui Li¹ and Si-Hong Zhou^{1,2*}

¹*Inner Mongolia Key Laboratory of Microscale Physics and Atom Manufacturing,*

School of Physical Science and Technology,

Inner Mongolia University, Hohhot 010021, China

²*Center for Quantum Physics and Technologies,*

Inner Mongolia University, Hohhot 010021, China

(Dated: April 2, 2026)

Abstract

We present a precise and systematic analysis of $D \rightarrow VV$ decays within the factorization-assisted topological-amplitude (FAT) approach, where D denotes the set $\{D^0, D^+, D_s^+\}$ and V represents the vector mesons ρ, K^*, ω , and ϕ . Given the limited current experimental data, the FAT approach serves as a available phenomenological framework for predicting charmed meson decays to both vector mesons. In this framework, incorporating flavor SU(3) symmetry breaking effects, we can express nonfactorizable contributions of different modes as a minimal set of universal parameters globally fitted to experimental data. Utilizing 36 experimental data points for $D \rightarrow VV$ decays, we precisely extract 10 nonfactorizable parameters associated with the C and E topological diagrams with $\chi^2/\text{d.o.f.} = 8.43$. We find that a large strong phase in the longitude E amplitude cause strong destructive interference with the C longitudinal component, yielding $f_{\parallel} > f_L$, contrary to the naive factorization predictions. Additionally, for modes processing exclusively by the E diagram, the amplitude hierarchy $|S| < |D|$ leads to a D -wave branching fraction larger than that of the S -wave. This explains recent observations that contradict S -wave dominance predictions. The predicted branching fractions and polarizations for 28 decay modes are consistent with existing experimental data. Unobserved modes, especially those with branching fractions of order $10^{-3} \sim 10^{-2}$, the D -wave dominated modes, and modes exhibiting $f_{\parallel} > f_L$, await measurement by BESIII, STCF, Belle II and LHCb.

* corresponding author: shzhou@imu.edu.cn

I. INTRODUCTION

Since 2003, BaBar [1] and Belle [2] have measured large transverse polarization fractions ($\sim 50\%$) in $B \rightarrow \phi K^*$, respectively, contradicting the fraction expectation of dominant longitudinal polarization fractions, $f_L = 1 - \mathcal{O}(m_V^2/m_B^2)$. Similar anomalies were observed in other penguin-dominated strangeness-changing decays, such as $B^+ \rightarrow \omega K^{*+}$, $B^+ \rightarrow K^{*+}$, and $B_s \rightarrow \phi\phi$, sparking extensive theoretical interest. Although transverse polarization fractions in the charm sector are not as heavily suppressed as in B decays, they still significantly deviate from naive factorization estimates. For instance, Mark III Collaboration reported a transverse branching fraction of $\mathcal{B}(D^0 \rightarrow \bar{K}^{*0}\rho^0)_T = (1.6 \pm 0.6)\%$, comparable to the total branching fraction of $\mathcal{B}(D^0 \rightarrow \bar{K}^{*0}\rho^0)_{\text{tot}} = (1.59 \pm 0.35)\%$ [3], and partial wave analysis yields S -, P - and D -wave components of $(3.1 \pm 0.6)\%$, $< 3 \times 10^{-3}$ and $(2.1 \pm 0.6)\%$, respectively. This hierarchy contradicts the naive prediction $|S|^2 > |P|^2 > |D|^2$. Subsequently, BES III found D -wave dominance in $D^0 \rightarrow K^{*-}\rho^+$, $\bar{K}^{*0}\rho^0$, $\rho^+\rho^-$ and P -wave dominance in $D_s^+ \rightarrow \bar{K}^{*0}\rho^+$, $K^{*-}\rho^0$ [4–6]. Additionally, the D -wave dominance in $D^0 \rightarrow \rho^0\rho^0$ was reported by FOCUS [7], with partial wave analyses further done in Ref. [8].

To understand these “polarization anomalies” in $D \rightarrow VV$ decays within QCD remains challenging due to the intermediate charm mass scale, m_c . Unlike B decays, where heavy quark expansion ($1/m_b$) enable successful applications of QCD factorization, perturbative QCD, and soft-collinear effective theory, the mass m_c is not sufficiently large to allow for such an expansion. Early studies of $D \rightarrow VV$ decays relied on naive factorization estimates [9–12], pole-dominance model [13], heavy quark effective Lagrangian combined with chiral perturbative theory [14], or model-independent symmetry based approaches, including flavor SU(3) symmetry [9] and broken flavor SU(3) symmetry models [15]. These studies typically focusing on only a few specific modes. Recent works have extended this to systematic analyses of all Cabibbo-favored and Singly Cabibbo-suppressed $D^0 \rightarrow VV$ decays using quark model with final state interactions (FSIs) [16], and all $D^0 \rightarrow VV$ decays have been studied in naive factorization [17]. While abundance data for $D \rightarrow PP$ and $D \rightarrow PV$ decays have enabled systematic phenomenological studies via topological diagram approach [17, 18], the FAT approach [19, 20], and quark model [21], $D - VV$ decays are experimentally more challenging. Consequently, the resulting scarcity and limited precision of data have prevented their study within the topological diagram approach. Leveraging current available data,

the FAT approach offers a viable framework to predict all $D_{(s)} - VV$ mode, encompassing Cabibbo-favored, Singly Cabibbo-suppressed, and Doubly Cabibbo-suppressed decays.

The FAT approach builds upon the conventional topological diagram approach [22, 23]. In the topological diagram approach, decay amplitudes are categorized into distinct topological diagrams according to electroweak interactions. As the weak interaction is factorized automatically from strong interaction due to their distant scales, the QCD effects including perturbative and nonperturbative contributions (including FSI), are effectively encapsulated within these topological amplitudes. Consequently, when these amplitudes (excluding the common factor $G_F/\sqrt{2}V_{\text{CKM}}$) are extracted directly from experimental data, they inherently contain all QCD effects. However, the conventional topological diagram approach relies on flavor SU(3) symmetry to reduce the number of free parameters so as to improve fit quality. It is well established that the SU(3) breaking effects can reach 20 – 30% in B decays [24, 25] and are expected to be even larger in D decays. This significant symmetry breaking limits the prediction power of the conventional diagrammatic approach. The FAT approach addresses this limitation by incorporating SU(3) breaking effects assisted by factorization. Specially, we factor out the form factors and decay constants from the topological diagram amplitudes. As a result, the remaining nonfactorizable contributions become universal across all decay modes and can be characterized by a minimal set of free parameters, determined through a global fit to all available experimental data.

The FAT framework was originally developed for charm meson decays [19, 20, 26], and later extended to B -meson decays by one of us (S.-H. Z.) and collaborators [24, 25, 27] (see [28] for a review). It has been applied to $D^0 - \bar{D}^0$ mixing [29], $K_S^0 - K_L^0$ asymmetries [30], CP violation in charm decays [31], and the extraction of the CKM phase γ from charmless two-body B decays [32]. Recent extensions include quasi-two-body B decays [33–36] and D decays [37, 38]. Notably, the FAT approach has successfully explained the “polarization anomalies” in $B \rightarrow VV$ decays [27] by predicting reduced branching fractions and longitudinal polarization fractions for color-suppressed decays and attributing large transverse polarization fractions observed in the penguin dominant modes to a single transverse amplitude. In this work, we apply the the FAT approach to systematically analyze $D \rightarrow VV$ decays. We aim to resolve the “polarization anomalies” in the charm sector and provide robust predictions as references for upcoming experimental measurements.

The remainder of this paper is organized as follows. In Sec. II, we introduce the theoretical

framework. Numerical results and detailed discussions are presented in Sec. III. Finally, our conclusions are summarized in Sec. IV.

II. FACTORIZATION AMPLITUDES FOR TOPOLOGICAL DIAGRAMS

In this section, we first introduce the decay amplitudes for $D \rightarrow VV$ decays in various bases, along with their expressions within naive factorization. We then proceed to analyze the three polarization amplitudes under the FAT framework.

A. Decay amplitude decomposition and naive factorization

For a D meson with four-momentum p_D decaying into two vector mesons $V_1(m_1, p_1, \eta^*)$ and $V_2(m_2, p_2, \epsilon^*)$ with polarization vectors η^* and ϵ^* , the decay amplitude, based on Lorentz decomposition, reads

$$\mathcal{A}_{D \rightarrow V_1 V_2} = i\eta^{*\mu} \epsilon^{*\nu} \left(g_{\mu\nu} S_1 - \frac{p_{D\mu} p_{D\nu}}{m_D^2} S_2 + i\epsilon_{\mu\nu\rho\sigma} \frac{p_1^\rho p_2^\sigma}{p_1 \cdot p_2} S_3 \right). \quad (1)$$

The amplitudes with definite helicity ($h = 0, +, -$) are expressed as

$$\begin{aligned} \mathcal{A}^0 &= \mathcal{A}[D \rightarrow V_1(p_1, \eta_0^*) V_2(p_2, \epsilon_0^*)] = i \frac{m_D^2}{2m_1 m_2} \left(S_1 - \frac{S_2}{2} \right), \\ \mathcal{A}^\pm &= \mathcal{A}[D \rightarrow V_1(p_1, \eta_\pm^*) V_2(p_2, \epsilon_\pm^*)] = i(S_1 \mp S_3). \end{aligned} \quad (2)$$

Within the naive factorization framework, the helicity amplitudes can be formally expressed as

$$\mathcal{A}^h = \frac{G_F}{\sqrt{2}} V_{CKM} \langle V_1^h | (\bar{c}q)_{V-A} | D \rangle \langle V_2^h | (\bar{q}q')_V | 0 \rangle, \quad (3)$$

By neglecting m_i^2 contributions, the three helicity amplitudes are explicitly given by

$$\begin{aligned} \mathcal{A}^0 &= i \frac{G_F}{\sqrt{2}} V_{CKM} f_2 m_D^2 A_0^{DV_1}(m_2^2), \\ \mathcal{A}^+ &= i \frac{G_F}{\sqrt{2}} V_{CKM} f_2 m_2 \left\{ -(m_D + m_1) A_1^{DV_1}(m_2^2) + (m_D - m_1) V^{DV_1}(m_2^2) \right\}, \\ \mathcal{A}^- &= i \frac{G_F}{\sqrt{2}} V_{CKM} f_2 m_2 \left\{ -(m_D + m_1) A_1^{DV_1}(m_2^2) - (m_D - m_1) V^{DV_1}(m_2^2) \right\}, \end{aligned} \quad (4)$$

where $A_0^{DV_1}(m_2^2)$, $A_1^{DV_1}(m_2^2)$ and $V^{DV_1}(m_2^2)$ denote the transition form factors, as defined in Refs. [10, 39]. Given the m_2/m_D suppression of \mathcal{A}^\pm relative to the \mathcal{A}^0 and the A_1 and V

cancellation, the amplitudes follow the hierarchy

$$\mathcal{A}^0 : \mathcal{A}^- : \mathcal{A}^+ = 1 : \frac{\Lambda_{\text{QCD}}}{m_c} : \left(\frac{\Lambda_{\text{QCD}}}{m_c} \right)^2. \quad (5)$$

In general, decay amplitudes admit several equivalent representations. Specially, the helicity amplitudes $\mathcal{A}^{0,+,-}$ relate to the spin amplitudes in the transversity basis ($\mathcal{A}^{L,\parallel,\perp}$) as follows,

$$\mathcal{A}_L = \mathcal{A}^0; \quad \mathcal{A}_\parallel = \frac{\mathcal{A}^+ + \mathcal{A}^-}{\sqrt{2}}; \quad \mathcal{A}_\perp = \frac{\mathcal{A}^+ - \mathcal{A}^-}{\sqrt{2}}. \quad (6)$$

In the transversity basis, the three amplitudes can be further simplified as

$$\begin{aligned} \mathcal{A}_L &= i \frac{G_F}{\sqrt{2}} V_{CKM} f_2 m_D^2 A_0^{DV_1}(m_2^2), \\ \mathcal{A}_\parallel &= -i G_F V_{CKM} f_2 m_2 (m_D + m_1) A_1^{DV_1}(m_2^2), \\ \mathcal{A}_\perp &= i G_F V_{CKM} f_2 m_2 (m_D - m_1) V^{DV_1}(m_2^2), \end{aligned} \quad (7)$$

As experimental data for $D \rightarrow VV$ decays are predominantly presented in terms of partial-wave (S, P, D) branching fractions, it is necessary to convert the transversity amplitudes into partial-wave amplitudes via

$$S = \frac{1}{\sqrt{3}}(-\mathcal{A}_0 + \sqrt{2}\mathcal{A}_\parallel); \quad P = \mathcal{A}_\perp; \quad D = \frac{1}{\sqrt{3}}(\sqrt{2}\mathcal{A}_0 + \mathcal{A}_\parallel). \quad (8)$$

Eqs.(7) and (8) reveal that, in the naive factorization approach, the polarization amplitude hierarchies satisfy $|\mathcal{A}_\parallel|^2 \geq |\mathcal{A}_0|^2 > |\mathcal{A}_\perp|^2$, and $|S|^2 \geq |P|^2 > |D|^2$ [17].

B. Polarization amplitudes within the FAT framework

The $D \rightarrow VV$ decay is a weak process induced primarily by the tree-level quark transition $c \rightarrow d(s) u \bar{d}(\bar{s})$. Although penguin contributions ($c \rightarrow u q \bar{q}$ with $q = u, d, s$) exist, they are neglected in branching fraction calculations due to suppression by both small Wilson coefficients and Cabibbo-Kobayashi-Maskawa (CKM) matrix elements. Based on the weak interaction, the tree-level topological diagrams for $D \rightarrow V_1 V_2$ decays are conventionally classified into four categories: (i) color-favored emission diagram T , (ii) color-suppressed emission diagram C , (iii) W -exchange diagram E , and (iv) W -annihilation diagram A , which are as illustrated in Fig. 1. Here, we factorize the weak interaction from strong interaction, thereby incorporating all perturbative and nonperturbative QCD corrections

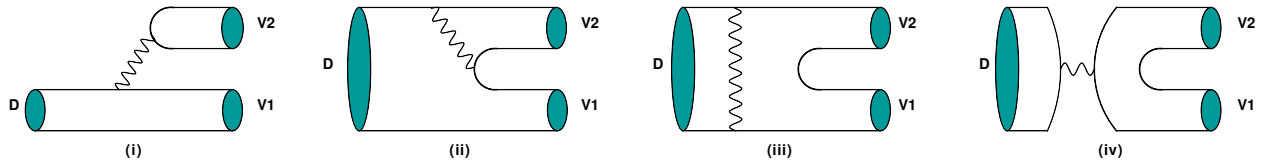


FIG. 1: Topological diagrams for $D \rightarrow V_1 V_2$ with the wave line representing a W boson: (i) the color-favored emission diagram T , (ii) the color-suppressed emission diagram C , (iii) the W -exchange diagram E , and (iv) W -annihilation diagram A .

into the topological diagrams. While the conventional topological diagram approach treats these four topological amplitudes as unknown parameters fitted under $SU(3)$ symmetry, the FAT approach explicitly accounts for $SU(3)$ breaking effects via factorization. In the following, we analyze the four topological amplitudes (T , C , E , and A) within the FAT framework.

Firstly, the T diagram is typically treated as factorizable. To minimize the number of free parameters, we directly adopt the naive factorization results, analogous to Eq.(7), including the relevant Wilson coefficients. The T amplitudes for the three polarization states are expressed as

$$\begin{aligned}
 T^0 &= i \frac{G_F}{\sqrt{2}} V_{\text{CKM}} a_1(\mu) m_D^2 f_2 A_0^{DV_1}(m_2^2), \\
 T^\parallel &= -i G_F V_{\text{CKM}} a_1(\mu) m_2 (m_D + m_1) f_2 A_1^{DV_1}(m_2^2), \\
 T^\perp &= i G_F V_{\text{CKM}} a_1(\mu) m_2 (m_D - m_1) f_2 V^{DV_1}(m_2^2),
 \end{aligned} \tag{9}$$

where $a_1(\mu) = C_2(\mu) + C_1(\mu)/3$ is the effective Wilson coefficients for four-quark operators. The scale parameter μ , representing the energy release, is treated as a single free parameter constrained to be below $m_c/2$. The terms $A_0^{DV_1}$, $A_1^{DV_1}$, and V^{DV_1} denote the transition form factors, and f_2 is the decay constant of the emitted vector meson. In contrast to the conventional diagrammatic approach, where describing the three decay amplitudes requires at least five free parameters (three magnitudes and two strong phase for T amplitudes) to be fitted from experimental data, our formulation introduces only one free parameter, μ , for all T amplitudes. Furthermore, $SU(3)$ breaking effects are naturally incorporated through the use of distinct decay constants and form factors for different decay modes.

The remaining three diagrams (C , E , A) are dominated by nonfactorizable contributions. For the C diagram, after factorizing out form factor and decay constant to account for

SU(3) breaking effects, the residual contribution is expected to be universal across different processes. We introduce two sets of unknown parameters, $\chi_C^{0(\parallel,\perp)}$ and $\phi_C^{0(\parallel,\perp)}$, representing the magnitudes and associate strong phases for each polarization amplitude, respectively. These amplitudes are expressed as

$$\begin{aligned} C^0 &= i \frac{G_F}{\sqrt{2}} V_{\text{CKM}} \chi_C^0 e^{i\phi_C^0} m_D^2 f_2 A_0^{DV_1}(m_2^2), \\ C^\parallel &= -i G_F V_{\text{CKM}} \chi_C^\parallel e^{i\phi_C^\parallel} m_2 (m_D + m_1) f_2 A_1^{DV_1}(m_2^2), \\ C^\perp &= i G_F V_{\text{CKM}} \chi_C^\perp e^{i\phi_C^\perp} m_2 (m_D - m_1) f_2 V^{DV_1}(m_2^2). \end{aligned} \quad (10)$$

Similarly, for the E diagram, we factorize the relevant meson decay constants to characterize SU(3) breaking effects. The polarized amplitudes are given by

$$\begin{aligned} E^0 &= i \frac{G_F}{\sqrt{2}} V_{\text{CKM}} \chi_E^0 e^{i\phi_E^0} m_D^2 f_D f_1 f_2 \frac{1}{f_\rho^2}, \\ E^\parallel &= -i G_F V_{\text{CKM}} \chi_E^\parallel e^{i\phi_E^\parallel} m_D (m_1 + m_2) f_D f_1 f_2 \frac{1}{f_\rho^2}, \\ E^\perp &= i G_F V_{\text{CKM}} \chi_E^\perp e^{i\phi_E^\perp} m_D^2 f_D f_1 f_2 \frac{1}{f_\rho^2}, \end{aligned} \quad (11)$$

where the parameters $\chi_E^{0,\parallel,\perp}$ are dimensionless quantities normalized to f_ρ^2 .

The A diagram amplitudes follow a parametrization similar to the E diagram, substituting the parameters $\chi_E^{0,\parallel,\perp}$ and $\phi_E^{0,\parallel,\perp}$ with $\chi_A^{0,\parallel,\perp}$ and $\phi_A^{0,\parallel,\perp}$,

$$\begin{aligned} A^0 &= i \frac{G_F}{\sqrt{2}} V_{\text{CKM}} \chi_A^0 e^{i\phi_A^0} m_D^2 f_D f_1 f_2 \frac{1}{f_\rho^2}, \\ A^\parallel &= -i G_F V_{\text{CKM}} \chi_A^\parallel e^{i\phi_A^\parallel} m_D (m_1 + m_2) f_D f_1 f_2 \frac{1}{f_\rho^2}, \\ A^\perp &= i G_F V_{\text{CKM}} \chi_A^\perp e^{i\phi_A^\perp} m_D^2 f_D f_1 f_2 \frac{1}{f_\rho^2}. \end{aligned} \quad (12)$$

Nevertheless, we neglect the A diagram in later analysis because its contribution is negligible. Attempting to include these parameters in our fitting program, we fail to obtain stable solutions due to the limited precision of current experimental data.

In total, we have 9 magnitudes and 9 strong phases, along with the scale parameter μ , to be fitted simultaneously to the the experimental data. With these fitted parameters, we can predict the branching fractions and two out of the three polarization fractions ($f_L, f_\parallel, f_\perp$)

for all $D_{\bar{q}} \rightarrow VV(\bar{q} = \bar{u}, \bar{d}, \bar{s})$ based on the standard definitions as follows

$$\begin{aligned}\Gamma &\equiv \frac{|\mathbf{p}|}{8\pi m_D^2} \frac{|\mathcal{A}_L|^2 + |\mathcal{A}_{\parallel}|^2 + |\mathcal{A}_{\perp}|^2 + |\overline{\mathcal{A}}_L|^2 + |\overline{\mathcal{A}}_{\parallel}|^2 + |\overline{\mathcal{A}}_{\perp}|^2}{2}, \\ &= \frac{|\mathbf{p}|}{8\pi m_D^2} \frac{|S|^2 + |P|^2 + |D|^2 + |\overline{S}|^2 + |\overline{P}|^2 + |\overline{D}|^2}{2},\end{aligned}\tag{13}$$

and

$$f_{L,\parallel,\perp}^D = \frac{\Gamma_{L,\parallel,\perp}}{\Gamma} = \frac{|\mathcal{A}_{L,\parallel,\perp}|^2}{|\mathcal{A}_L|^2 + |\mathcal{A}_{\parallel}|^2 + |\mathcal{A}_{\perp}|^2},\tag{14}$$

respectively.

III. NUMERICAL RESULTS AND DISCUSSIONS

A. Input parameters

The input parameters are categorized into: (i) CKM matrix elements and Wilson coefficients; (ii) meson masses and decay constants; and (iii) $D_{(s)} \rightarrow V$ transition form factors. The CKM matrix elements are taken from the PDG [40], and the Wilson coefficients,

TABLE I: Masses m_V and decay constant of mesons (in units of MeV).

Meson	Mass	Decay Constant
D^{\pm}	1869.66	212.0 ± 0.7
D^0	1864.84	212.0 ± 0.7
D_s	1968.35	249.9 ± 0.5
ρ	775.26	223.7 ± 11.2
ω	782.66	182.4 ± 9.1
ϕ	1019.46	236.3 ± 11.8
K^{*+}	891.67	214.7 ± 10.7
K^{*0}	895.55	214.7 ± 10.7

$C_{1(2)}(\mu)$, for D -meson decays follow Eqs. (B1) and (B2) in the Appendix of Ref. [26]. The masses and decay constants of the D mesons and vector mesons are listed in Table. I. Specifically, all masses and $D_{(s)}$ meson decay constants are provided by the PDG [40]. The decay constants of vector mesons (ρ , ω , ϕ , K^*) have not been measured experimentally but are

calculated in several theoretical approaches, such as quark model [41], covariant light front approach [42], light-cone sum rules [43, 44], QCD sum rules [45, 45], etc. Given the variations among these theoretical results, we adopt the numerical values shown in the Table. I and keep a 5% uncertainty to them.

The transition form factors of $D \rightarrow V$ are also unmeasured. We adopt values from Ref. [10], calculated at zero recoil momentum ($q^2 = 0$) in Ref. [39] using relativistic oscillator wave functions. The corresponding values at $q^2 = 0$ are presented in Table. II and a 10% uncertainties is assigned to these form factors. Their q^2 dependence is parameterized using the nearest pole dominance form [10, 39] as follows

$$F_i(q^2) = \frac{F_i(0)}{1 - q^2/m_{\text{pole}}^2}, \quad (15)$$

where F_i represents form factors A_0 , A_1 or V , and m_{pole} is the mass of the corresponding pole state, which are displayed in Table III from Ref. [10, 39]. Specifically, we use $m(0^-, \bar{d}c)$ for $A_0^{D\rho, D\omega, D_s K^*}$ and $m(0^-, \bar{s}c)$ for $A_0^{DK^*, D_s \phi}$; $m(1^+, \bar{d}c)$ for $A_1^{D\rho, D\omega, D_s K^*}$ and $m(1^+, \bar{s}c)$ for $A_1^{DK^*, D_s \phi}$; $m(1^-, \bar{d}c)$ for $V^{D\rho, D\omega, D_s K^*}$ and $m(1^-, \bar{s}c)$ for $V^{DK^*, D_s \phi}$.

TABLE II: Form factors at zero recoil momentum for $D \rightarrow V$ transitions [10].

	$V^{D \rightarrow \rho}$	$V^{D \rightarrow K^*}$	$V^{D_s \rightarrow K^*}$	$V^{D \rightarrow \omega}$	$V^{D_s \rightarrow \phi}$
$V(0)$	1.225	1.226	1.250	1.236	1.319
	$A_0^{D \rightarrow \rho}$	$A_0^{D \rightarrow K^*}$	$A_0^{D_s \rightarrow K^*}$	$A_0^{D \rightarrow \omega}$	$A_0^{D_s \rightarrow \phi}$
$A_0(0)$	0.669	0.733	0.634	0.669	0.700
	$A_1^{D \rightarrow \rho}$	$A_1^{D \rightarrow K^*}$	$A_1^{D_s \rightarrow K^*}$	$A_1^{D \rightarrow \omega}$	$A_1^{D_s \rightarrow \phi}$
$A_1(0)$	0.775	0.880	0.717	0.772	0.820

TABLE III: Values of pole masses used in Eq.(15) (in units of GeV).

Current	$m(0^-)$	$m(1^-)$	$m(0^+)$	$m(1^+)$
$\bar{d}c$	1.87	2.01	2.47	2.42
$\bar{s}c$	1.97	2.11	2.60	2.53

B. The nonfactorizable parameters

The free parameters in the topological diagram amplitudes defined in Eqs. (9-12) consist of 19 parameters: $\chi_C^{0,\parallel,\perp}$, $\chi_E^{0,\parallel,\perp}$, and $\chi_A^{0,\parallel,\perp}$, along with their associated strong phases $\phi_E^{0,\parallel,\perp}$, $\phi_C^{0,\parallel,\perp}$, and $\phi_A^{0,\parallel,\perp}$, as well as the factorization scale μ [appearing in the Wilson coefficients $a_1(\mu)$ of the T diagram amplitude in Eq.(9)]. In the experimental sector, the total and partial branching fractions of $D \rightarrow VV$ have been measured by BESIII [4–6, 46–49], LHCb [50, 51], CLEO-c [8], FOCUS [7] and Mark III Collaborations [3], where all measurements of D^+ and D_s^+ decays are provided by BESIII. The data used in the global fit are listed in Tables IV-VI, taken from the PDG [40] and recent BESIII measurements. In total, 36 data points are available to constrain the 19 free parameters. However, we observe that the number of free parameters is too large to be precisely determined by the limited experimental data, thereby diminishing the predictive power of the FAT approach.

Given the very small values of χ_E^\perp found in preliminary fit, we neglect the parameter χ_E^\perp and its associated strong phase ϕ_E^\perp . Moreover, as the A diagram amplitude is typically smaller than that of the E diagram, we ignore the A diagram contributions entirely. Consequently, by setting $\chi_E^\perp = \chi_A^0 = \chi_A^\parallel = \chi_A^\perp = 0$, $\phi_E^\perp = \phi_A^0 = \phi_A^\parallel = \phi_A^\perp = 0$, the number of free parameters is reduced to 11. These remaining parameters are subsequently determined through a global fit to 36 experimental data points. The best-fitted values, together with their corresponding uncertainties, are list as follows,

$$\begin{aligned}
\mu &= 465.14 \pm 0.12 \text{ MeV}, \\
\chi_C^0 &= 0.55 \pm 0.03, & \phi_C^0 &= 0.87 \pm 0.10, \\
\chi_C^\parallel &= 0.45 \pm 0.03, & \phi_C^\parallel &= 0.77 \pm 0.11, \\
\chi_C^\perp &= 0.37 \pm 0.02, & \phi_C^\perp &= 0.36 \pm 0.04, \\
\chi_E^0 &= 0.24 \pm 0.07, & \phi_E^0 &= 2.23 \pm 0.30, \\
\chi_E^\parallel &= 0.25 \pm 0.03, & \phi_E^\parallel &= 0.23 \pm 0.21,
\end{aligned} \tag{16}$$

with $\chi^2/\text{d.o.f.} = 8.43$. These obtained nonfactorizable parameters are highly precise, with the exception of the strong phase ϕ_E^\parallel . This large uncertainty arises because the E amplitude always appears alongside the T or C amplitude, and the transverse polarization branching fraction is smaller than that of longitude polarization. Consequently, no sufficiently precise data involving the E amplitude exist to constrain the strong phase ϕ_E^\parallel .

At the factorization scale $\mu = 465.14$ MeV, the Wilson coefficient is $a_1 = -0.47$ in the T amplitude, which corresponds to the factorizable contribution of the T diagram. We find the hierarchies $|C^0| > |T^0| > |E^0|$ and $|T^{\parallel(\perp)}| \sim |C^{\parallel(\perp)}| > |E^{\parallel(\perp)}|$. This indicates that the nonfactorizable contribution of the C diagram is comparable to the factorizable contributions of the T diagram. This suggests the potential need to include nonfactorizable contributions for the T diagram by inducing five additional parameters $\chi_T^{0,\parallel,\perp}$ and strong phases $\phi_T^{\parallel,\perp}$. However, obtaining reliable results for such a large number of parameters is difficult given the limited experimental data.

using the specific decay modes $D^0 \rightarrow \bar{K}^{*-}\rho^+$ and $D^0 \rightarrow \rho^0\bar{K}^{*0}$ as examples, we examine the hierarchies of polarization components (0, \parallel , \perp) and partial-wave contributions (S, P, D) in the T, C and E amplitudes:

$$\begin{aligned} |T_{D^0 \rightarrow K^{*-}\rho^+}^0| : |T_{D^0 \rightarrow K^{*-}\rho^+}^{\parallel}| : |T_{D^0 \rightarrow K^{*-}\rho^+}^{\perp}| &= 1 : 0.97 : 0.50, \\ |C_{D^0 \rightarrow \rho^0\bar{K}^{*0}}^0| : |C_{D^0 \rightarrow \rho^0\bar{K}^{*0}}^{\parallel}| : |C_{D^0 \rightarrow \rho^0\bar{K}^{*0}}^{\perp}| &= 1 : 0.81 : 0.47, \\ |E_{D^0 \rightarrow K^{*-}\rho^+}^0| : |E_{D^0 \rightarrow K^{*-}\rho^+}^{\parallel}| &= 1 : 1.31, \end{aligned} \quad (17)$$

and

$$\begin{aligned} |T_{D^0 \rightarrow K^{*-}\rho^+}^S| : |T_{D^0 \rightarrow K^{*-}\rho^+}^P| : |T_{D^0 \rightarrow K^{*-}\rho^+}^D| &= 1 : 0.37 : 0.19, \\ |C_{D^0 \rightarrow \rho^0\bar{K}^{*0}}^S| : |C_{D^0 \rightarrow \rho^0\bar{K}^{*0}}^P| : |C_{D^0 \rightarrow \rho^0\bar{K}^{*0}}^D| &= 1 : 0.37 : 0.28, \\ |E_{D^0 \rightarrow K^{*-}\rho^+}^S| : |E_{D^0 \rightarrow K^{*-}\rho^+}^D| &= 1 : 1.36, \end{aligned} \quad (18)$$

respectively.

The hierarchies in Eq.(17) indicate that the polarization amplitudes satisfy $|\mathcal{A}^0| > |\mathcal{A}^{\parallel}| > |\mathcal{A}^{\perp}|$ for the T amplitude, and particularly for the C amplitude. This differs from the naive factorization prediction, $|\mathcal{A}^{\parallel}| \geq |\mathcal{A}^0| > |\mathcal{A}^{\perp}|$. This discrepancy arises because the C diagram contribution is primarily nonfactorizable, which cannot be accurately calculated within the naive factorization approach. Our result implies that the longitudinal polarization f_L remains dominant in decay modes not involving the E amplitude. For decays involving interference between T and E , or C and E amplitudes, the strong phases $\phi_{E,C}^{0,\parallel}$ determine the interference pattern, can potentially resulting in $f_L < f_{\parallel}$.

Regarding partial-wave amplitudes, Eq.(18) shows that $|S| > |P| > |D|$ for the T and C diagrams. Thus, the S -wave contribution is dominant. This is attributed to the definition in Eq.(8), where \mathcal{A}^0 and \mathcal{A}^{\parallel} exhibit constructive interference for the S -wave amplitude but

destructive interference for the D wave. However, the hierarchy is reversed for the E diagram (e.g., $|S| < |D|$) due to the large strong phase difference $|\phi_E^0 - \phi_E^\parallel|$. The hierarchy of $|S| < |D|$ for E amplitudes can lead to a larger D -wave branching fraction than that of the S -wave in the decays involving the E diagram, contrary to the naive factorization prediction of S -wave dominance.

C. Branching fractions of $D \rightarrow VV$ decays

Our numerical predictions for the branching fractions of 28 decay modes of D meson are collected in Tables IV-VII, organized by decay type: Cabibbo-favored (CF, Table IV), Singly Cabibbo-suppressed (SCS, Tables V-VI), and Doubly Cabibbo-suppressed (DCS, Table VII). In each table, the first column lists the decay modes, followed by the total branching fraction and its partial wave components (S -waves, P -waves, and D -waves). The second column identifies the relevant topological diagram amplitudes (T , C , E , and A) for the convenience of the subsequent discussion. The theoretical results, denoted as “ \mathcal{B}_{FAT} ”, appear in the final column. The quoted uncertainties correspond to: (i) variations in the nonperturbative parameters of Eq. (16); (ii) a 10% variation in the form factors; (iii) a 5% variation in the unmeasured decay constants. Among these, the form factor uncertainty dominates. For comparison, we also list the experimental data (“ \mathcal{B}_{exp} ”), which constitute the dataset used in our global fit. We explicitly exclude the $D^0 \rightarrow \bar{K}^{*0} K^{*0}$ channel from the fit. Including this mode would result in a χ^2 contribution of approximately 484 from this single mode alone, significantly compromising the global fit quality. This discrepancy arise because, at the quark level, the decay amplitude is governed by the E diagram with a CKM structure of $V_{cd}^* V_{ud} + V_{cs}^* V_{us}$. Due to the unitarity of the CKM matrix, these two terms undergo significant cancellation, leading to a theoretically suppressed branching fraction that fall well short of the the experimental measurement $\mathcal{B}(D^0 \rightarrow \bar{K}^{*0} K^{*0}) = (0.88 \pm 0.04) \times 10^{-3}$ [40].

A comparison of the values in the last two columns indicates that our results are consistent with the measured CF and SCS modes within uncertainties, with the exception of the P -wave branching fractions for $D_s^+ \rightarrow K^{*0} \rho^+$ and $D^0 \rightarrow \rho^- \rho^+$ decays. These two modes contribute significantly to the total χ^2 , yielding values of approximately 45 for $D_s^+ \rightarrow K^{*0} \rho^+$ and 22 for $D^0 \rightarrow \rho^- \rho^+$. Since the E^\perp is not included in our analysis, these two modes receive contributions only from the T diagram, corresponding to predictions made using naive factorization.

TABLE IV: Total and partial waves (S , P , and D) branching fractions for Cabibbo-favored $D \rightarrow VV$ decays, given in units of percentage. Our theoretical predictions, denoted as \mathcal{B}_{FAT} , including uncertainties arising from the fitted parameters, form factors and decay constants, respectively. These are compared with experimental data, \mathcal{B}_{exp} . The second column indicates the topological diagram amplitudes, T, C, E, A , contributing to each mode.

Modes	Amplitudes	\mathcal{B}_{exp}	\mathcal{B}_{FAT}
$D \rightarrow V_1 V_2$	$V_{cs}^* V_{ud}$		
$D^0 \rightarrow K^{*-} \rho^+$	$T + E$	6.5 ± 2.5	$4.23 \pm 0.82 \pm 0.50 \pm 0.28$
$D^0 \rightarrow K^{*-} \rho^+(S)$		1.4 ± 0.4	$2.07 \pm 0.51 \pm 0.36 \pm 0.30$
$D^0 \rightarrow K^{*-} \rho^+(P)$		0.9 ± 0.2	$0.46 \pm 0.02 \pm 0.09 \pm 0.05$
$D^0 \rightarrow K^{*-} \rho^+(D)$		2.9 ± 0.8	$1.70 \pm 0.50 \pm 0.34 \pm 0.20$
$D^0 \rightarrow \rho^0 \bar{K}^{*0}$	$\frac{1}{\sqrt{2}}(C - E)$	1.52 ± 0.08	$1.65 \pm 0.40 \pm 0.22 \pm 0.17$
$D^0 \rightarrow \rho^0 \bar{K}^{*0}(S)$		0.8 ± 0.12	$0.68 \pm 0.23 \pm 0.16 \pm 0.09$
$D^0 \rightarrow \rho^0 \bar{K}^{*0}(P)$		0.28 ± 0.03	$0.25 \pm 0.02 \pm 0.05 \pm 0.03$
$D^0 \rightarrow \rho^0 \bar{K}^{*0}(D)$		0.98 ± 0.1	$0.72 \pm 0.27 \pm 0.12 \pm 0.10$
$D^0 \rightarrow \omega \bar{K}^{*0}$	$\frac{1}{\sqrt{2}}(C + E)$	1.1 ± 0.5	$3.63 \pm 0.43 \pm 0.34 \pm 0.44$
$D^0 \rightarrow \omega \bar{K}^{*0}(S)$			$3.01 \pm 0.40 \pm 0.33 \pm 0.35$
$D^0 \rightarrow \omega \bar{K}^{*0}(P)$			$0.25 \pm 0.02 \pm 0.05 \pm 0.02$
$D^0 \rightarrow \omega \bar{K}^{*0}(D)$			$0.37 \pm 0.18 \pm 0.04 \pm 0.08$
$D^+ \rightarrow \bar{K}^{*0} \rho^+$	$T + C$	6.23 ± 0.27	$6.32 \pm 1.05 \pm 0.66 \pm 0.45$
$D^+ \rightarrow \bar{K}^{*0} \rho^+(S)$		6.05 ± 0.30	$5.61 \pm 0.99 \pm 0.57 \pm 0.40$
$D^+ \rightarrow \bar{K}^{*0} \rho^+(P)$		0.173 ± 0.026	$0.16 \pm 0.03 \pm 0.03 \pm 0.01$
$D^+ \rightarrow \bar{K}^{*0} \rho^+(D)$			$0.55 \pm 0.29 \pm 0.23 \pm 0.05$
$D_s^+ \rightarrow \phi \rho^+$	T	3.98 ± 0.39	$4.55 \pm 0.19 \pm 0.58 \pm 0.46$
$D_s^+ \rightarrow \phi \rho^+(S)$		3.32 ± 0.35	$3.85 \pm 0.16 \pm 0.55 \pm 0.38$
$D_s^+ \rightarrow \phi \rho^+(P)$		0.63 ± 0.13	$0.53 \pm 0.02 \pm 0.11 \pm 0.05$
$D_s^+ \rightarrow \phi \rho^+(D)$			$0.17 \pm 0.01 \pm 0.12 \pm 0.02$
$D_s^+ \rightarrow K^{*+} \bar{K}^{*0}$	$C + A$	5.93 ± 0.88	$5.07 \pm 0.36 \pm 0.67 \pm 0.51$
$D_s^+ \rightarrow K^{*+} \bar{K}^{*0}(S)$		5.01 ± 0.92	$4.12 \pm 0.34 \pm 0.58 \pm 0.41$
$D_s^+ \rightarrow K^{*+} \bar{K}^{*0}(P)$		1.10 ± 0.19	$0.56 \pm 0.06 \pm 0.11 \pm 0.06$
$D_s^+ \rightarrow K^{*+} \bar{K}^{*0}(D)$		0.65 ± 0.16	$0.40 \pm 0.11 \pm 0.20 \pm 0.04$

TABLE V: Same as Table IV for singly Cabibbo-suppressed $D^0 \rightarrow VV$ decays in units of 10^{-3} .

Modes	Amplitudes	\mathcal{B}_{exp}	\mathcal{B}_{FAT}
$D \rightarrow V_1 V_2$	$V_{cd}^* V_{ud}$ or $V_{cs}^* V_{us}$		
$D^0 \rightarrow \rho^- \rho^+$	$T + E$	7.81 ± 1.14	$2.67 \pm 0.54 \pm 0.30 \pm 0.21$
$D^0 \rightarrow \rho^- \rho^+(S)$		1.20 ± 0.40	$1.08 \pm 0.31 \pm 0.18 \pm 0.13$
$D^0 \rightarrow \rho^- \rho^+(P)$		1.80 ± 0.30	$0.39 \pm 0.02 \pm 0.08 \pm 0.04$
$D^0 \rightarrow \rho^- \rho^+(D)$		3.30 ± 0.50	$1.20 \pm 0.35 \pm 0.21 \pm 0.09$
$D^0 \rightarrow \rho^0 \rho^0$	$\frac{1}{2}(E - C)$	1.33 ± 0.35	$0.49 \pm 0.13 \pm 0.07 \pm 0.04$
$D^0 \rightarrow \rho^0 \rho^0(S)$		0.18 ± 0.13	$0.18 \pm 0.07 \pm 0.04 \pm 0.03$
$D^0 \rightarrow \rho^0 \rho^0(P)$		0.53 ± 0.13	$0.061 \pm 0.006 \pm 0.012 \pm 0.006$
$D^0 \rightarrow \rho^0 \rho^0(D)$		0.62 ± 0.3	$0.26 \pm 0.09 \pm 0.04 \pm 0.02$
$D^0 \rightarrow K^{*-} K^{*+}$	$T + E$		$1.58 \pm 0.28 \pm 0.19 \pm 0.19$
$D^0 \rightarrow K^{*-} K^{*+}(S)$			$0.85 \pm 0.19 \pm 0.15 \pm 0.08$
$D^0 \rightarrow K^{*-} K^{*+}(P)$			$0.22 \pm 0.01 \pm 0.04 \pm 0.02$
$D^0 \rightarrow K^{*-} K^{*+}(D)$			$0.52 \pm 0.16 \pm 0.12 \pm 0.13$
$D^0 \rightarrow \rho^0 \phi$	$\frac{1}{\sqrt{2}}C$	1.56 ± 0.13	$1.13 \pm 0.08 \pm 0.14 \pm 0.11$
$D^0 \rightarrow \rho^0 \phi(S)$		1.40 ± 0.10	$0.92 \pm 0.08 \pm 0.13 \pm 0.09$
$D^0 \rightarrow \rho^0 \phi(P)$		0.081 ± 0.039	$0.149 \pm 0.015 \pm 0.030 \pm 0.015$
$D^0 \rightarrow \rho^0 \phi(D)$		0.085 ± 0.028	$0.053 \pm 0.019 \pm 0.032 \pm 0.005$
$D^0 \rightarrow \omega \phi$	$\frac{1}{\sqrt{2}}C$	0.648 ± 0.104	$1.066 \pm 0.074 \pm 0.135 \pm 0.107$
$D^0 \rightarrow \omega \phi(S)$			$0.873 \pm 0.073 \pm 0.124 \pm 0.087$
$D^0 \rightarrow \omega \phi(P)$			$0.141 \pm 0.014 \pm 0.028 \pm 0.014$
$D^0 \rightarrow \omega \phi(D)$			$0.051 \pm 0.018 \pm 0.031 \pm 0.005$
$D^0 \rightarrow \omega \rho^0$	$-E$		$0.77 \pm 0.19 \pm 0.08 \pm 0.08$
$D^0 \rightarrow \omega \rho^0(S)$			$0.35 \pm 0.14 \pm 0.08 \pm 0.03$
$D^0 \rightarrow \omega \rho^0(P)$			$0.0019 \pm 0.0002 \pm 0.0027 \pm 0.0014$
$D^0 \rightarrow \omega \rho^0(D)$			$0.42 \pm 0.17 \pm 0.02 \pm 0.07$
$D^0 \rightarrow \omega \omega$	$\frac{1}{2}(C + E)$		$0.71 \pm 0.09 \pm 0.07 \pm 0.10$
$D^0 \rightarrow \omega \omega(S)$			$0.58 \pm 0.08 \pm 0.06 \pm 0.08$
$D^0 \rightarrow \omega \omega(P)$			$0.041 \pm 0.004 \pm 0.008 \pm 0.004$
$D^0 \rightarrow \omega \omega(D)$			$0.09 \pm 0.041 \pm 0.01 \pm 0.02$

TABLE VI: Same as Table IV for singly Cabibbo-suppressed $D_{(s)}^+ \rightarrow VV$ decays in units of 10^{-3} .

Modes	Amplitudes	\mathcal{B}_{exp}	\mathcal{B}_{FAT}
$D \rightarrow V_1 V_2$	$V_{cd}^* V_{ud}$ or $V_{cs}^* V_{us}$		
$D^+ \rightarrow \rho^0 \rho^+$	$-\frac{1}{\sqrt{2}}(T + C)$		$1.81 \pm 0.30 \pm 0.26 \pm 0.18$
$D^+ \rightarrow \rho^0 \rho^+(S)$			$1.53 \pm 0.27 \pm 0.22 \pm 0.15$
$D^+ \rightarrow \rho^0 \rho^+(P)$			$0.07 \pm 0.01 \pm 0.01 \pm 0.01$
$D^+ \rightarrow \rho^0 \rho^+(D)$			$0.21 \pm 0.10 \pm 0.09 \pm 0.02$
$D^+ \rightarrow \bar{K}^{*0} K^{*+}$	T		$4.22 \pm 0.18 \pm 0.53 \pm 0.42$
$D^+ \rightarrow \bar{K}^{*0} K^{*+}(S)$			$3.61 \pm 0.15 \pm 0.52 \pm 0.36$
$D^+ \rightarrow \bar{K}^{*0} K^{*+}(P)$			$0.54 \pm 0.02 \pm 0.11 \pm 0.05$
$D^+ \rightarrow \bar{K}^{*0} K^{*+}(D)$			$0.060 \pm 0.003 \pm 0.065 \pm 0.006$
$D^+ \rightarrow \omega \rho^+$	$\frac{1}{\sqrt{2}}(T + C + 2A)$		$1.52 \pm 0.24 \pm 0.16 \pm 0.12$
$D^+ \rightarrow \omega \rho^+(S)$			$1.27 \pm 0.21 \pm 0.14 \pm 0.10$
$D^+ \rightarrow \omega \rho^+(P)$			$0.10 \pm 0.02 \pm 0.04 \pm 0.02$
$D^+ \rightarrow \omega \rho^+(D)$			$0.15 \pm 0.07 \pm 0.05 \pm 0.01$
$D^+ \rightarrow \rho^+ \phi$	C		$5.88 \pm 0.41 \pm 0.74 \pm 0.59$
$D^+ \rightarrow \rho^+ \phi(S)$			$4.82 \pm 0.40 \pm 0.69 \pm 0.48$
$D^+ \rightarrow \rho^+ \phi(P)$			$0.78 \pm 0.08 \pm 0.16 \pm 0.08$
$D^+ \rightarrow \rho^+ \phi(D)$			$0.28 \pm 0.10 \pm 0.17 \pm 0.03$
$D_s^+ \rightarrow K^{*0} \rho^+$	$T + A$	3.95 ± 0.39	$2.63 \pm 0.11 \pm 0.33 \pm 0.26$
$D_s^+ \rightarrow K^{*0} \rho^+(S)$		1.41 ± 0.24	$2.06 \pm 0.09 \pm 0.29 \pm 0.21$
$D_s^+ \rightarrow K^{*0} \rho^+(P)$		2.53 ± 0.31	$0.43 \pm 0.02 \pm 0.09 \pm 0.04$
$D_s^+ \rightarrow K^{*0} \rho^+(D)$			$0.138 \pm 0.006 \pm 0.080 \pm 0.014$
$D_s^+ \rightarrow K^{*+} \rho^0$	$\frac{1}{\sqrt{2}}(A - C)$		$1.46 \pm 0.11 \pm 0.20 \pm 0.15$
$D_s^+ \rightarrow K^{*+} \rho^0(S)$			$1.17 \pm 0.09 \pm 0.17 \pm 0.12$
$D_s^+ \rightarrow K^{*+} \rho^0(P)$		0.42 ± 0.17	$0.14 \pm 0.01 \pm 0.03 \pm 0.01$
$D_s^+ \rightarrow K^{*+} \rho^0(D)$			$0.16 \pm 0.04 \pm 0.07 \pm 0.02$
$D_s^+ \rightarrow K^{*+} \omega$	$\frac{1}{\sqrt{2}}(C + A)$		$0.98 \pm 0.07 \pm 0.13 \pm 0.10$
$D_s^+ \rightarrow K^{*+} \omega(S)$			$0.78 \pm 0.06 \pm 0.11 \pm 0.08$
$D_s^+ \rightarrow K^{*+} \omega(P)$			$0.09 \pm 0.01 \pm 0.02 \pm 0.01$
$D_s^+ \rightarrow K^{*+} \omega(D)$			$0.10 \pm 0.03 \pm 0.05 \pm 0.01$
$D_s^+ \rightarrow \phi K^{*+}$	$T + C + A$		$1.26 \pm 0.20 \pm 0.15 \pm 0.10$
$D_s^+ \rightarrow \phi K^{*+}(S)$			$1.11 \pm 0.19 \pm 0.13 \pm 0.09$
$D_s^+ \rightarrow \phi K^{*+}(P)$			$0.04 \pm 0.01 \pm 0.01 \pm 0.01$
$D_s^+ \rightarrow \phi K^{*+}(D)$			$0.10 \pm 0.05 \pm 0.05 \pm 0.01$

TABLE VII: Same as Table IV for doubly Cabibbo-suppressed $D \rightarrow VV$ decays in units of 10^{-4} .

Modes	Amplitudes	\mathcal{B}_{FAT}
$D \rightarrow V_1 V_2$	$V_{cd}^* V_{us}$	
$D^0 \rightarrow \rho^- K^{*+}$	$T + E$	$1.24 \pm 0.23 \pm 0.14 \pm 0.13$
$D^0 \rightarrow \rho^- K^{*+}(S)$		$0.55 \pm 0.14 \pm 0.09 \pm 0.06$
$D^0 \rightarrow \rho^- K^{*+}(P)$		$0.23 \pm 0.01 \pm 0.05 \pm 0.02$
$D^0 \rightarrow \rho^- K^{*+}(D)$		$0.46 \pm 0.14 \pm 0.09 \pm 0.07$
$D^0 \rightarrow K^{*0} \rho^0$	$\frac{1}{\sqrt{2}}(C - E)$	$0.47 \pm 0.11 \pm 0.06 \pm 0.05$
$D^0 \rightarrow K^{*0} \rho^0(S)$		$0.19 \pm 0.07 \pm 0.04 \pm 0.03$
$D^0 \rightarrow K^{*0} \rho^0(P)$		$0.07 \pm 0.01 \pm 0.01 \pm 0.01$
$D^0 \rightarrow K^{*0} \rho^0(D)$		$0.20 \pm 0.08 \pm 0.04 \pm 0.03$
$D^0 \rightarrow K^{*0} \omega$	$\frac{1}{\sqrt{2}}(C + E)$	$1.03 \pm 0.12 \pm 0.10 \pm 0.12$
$D^0 \rightarrow K^{*0} \omega(S)$		$0.86 \pm 0.12 \pm 0.09 \pm 0.10$
$D^0 \rightarrow K^{*0} \omega(P)$		$0.07 \pm 0.01 \pm 0.01 \pm 0.01$
$D^0 \rightarrow K^{*0} \omega(D)$		$0.11 \pm 0.05 \pm 0.01 \pm 0.02$
$D^+ \rightarrow K^{*0} \rho^+$	$C + A$	$3.17 \pm 0.22 \pm 0.41 \pm 0.32$
$D^+ \rightarrow K^{*0} \rho^+(S)$		$2.59 \pm 0.21 \pm 0.37 \pm 0.26$
$D^+ \rightarrow K^{*0} \rho^+(P)$		$0.37 \pm 0.04 \pm 0.07 \pm 0.04$
$D^+ \rightarrow K^{*0} \rho^+(D)$		$0.21 \pm 0.06 \pm 0.11 \pm 0.02$
$D^+ \rightarrow \rho^0 K^{*+}$	$\frac{1}{\sqrt{2}}(A - T)$	$1.50 \pm 0.06 \pm 0.18 \pm 0.15$
$D^+ \rightarrow \rho^0 K^{*+}(S)$		$1.17 \pm 0.05 \pm 0.17 \pm 0.12$
$D^+ \rightarrow \rho^0 K^{*+}(P)$		$0.29 \pm 0.01 \pm 0.06 \pm 0.03$
$D^+ \rightarrow \rho^0 K^{*+}(D)$		$0.037 \pm 0.002 \pm 0.030 \pm 0.004$
$D^+ \rightarrow \omega K^{*+}$	$\frac{1}{\sqrt{2}}(T + A)$	$1.47 \pm 0.06 \pm 0.18 \pm 0.15$
$D^+ \rightarrow \omega K^{*+}(S)$		$1.15 \pm 0.05 \pm 0.16 \pm 0.11$
$D^+ \rightarrow \omega K^{*+}(P)$		$0.29 \pm 0.01 \pm 0.06 \pm 0.03$
$D^+ \rightarrow \omega K^{*+}(D)$		$0.036 \pm 0.002 \pm 0.029 \pm 0.004$
$D_s^+ \rightarrow K^{*0} K^{*+}$	$T + C$	$0.82 \pm 0.13 \pm 0.12 \pm 0.08$
$D_s^+ \rightarrow K^{*0} K^{*+}(S)$		$0.70 \pm 0.12 \pm 0.10 \pm 0.07$
$D_s^+ \rightarrow K^{*0} K^{*+}(P)$		$0.037 \pm 0.007 \pm 0.007 \pm 0.004$
$D_s^+ \rightarrow K^{*0} K^{*+}(D)$		$0.08 \pm 0.04 \pm 0.04 \pm 0.01$

Additionally, pure annihilation processes, $D_s^+ \rightarrow \rho^+\omega$, $D^+ \rightarrow \bar{K}^{*0}K^{*+}$, and $D_s^+ \rightarrow K^{*+}\rho^0$, mediated exclusively by the A diagram are excluded from our predictions due to the neglect of A diagram contribution. Kinematically forbidden decays, $D^0 \rightarrow \bar{K}^{*0}\phi$, $K^{*0}\phi$, $\phi\phi$ and $D^+ \rightarrow \bar{K}^{*+}\phi$, are also omitted. Predictions for unmeasured decay modes in the FAT approach remain to be tested against future experimental data.

In the following, we analyze the branching fraction values of specific modes listed in the Tables IV-VII. The total branching fractions of these modes are dominated by contributions from the T and C diagrams. The partial wave results are discussed explicitly for each mode.

We begin with modes where the D -wave branching fraction exceeds the S -wave, such as $D^0 \rightarrow \rho^0\bar{K}^{*0}$, $D^0 \rightarrow \rho^0\rho^0$, and $D^0 \rightarrow K^{*0}\rho^0$, which involve the amplitudes $\frac{1}{\sqrt{2}}(C - E)$, as well as $D^0 \rightarrow \omega\rho^0$ involving the E amplitude. In these decays, the C and the E amplitudes interfere destructively for both the S -wave and the D -wave branching fractions. Because the D -wave amplitude for the E diagram is significantly larger than that for the C diagram, the combined D -wave term $\frac{1}{\sqrt{2}}(C - E)$ approximates $-\frac{1}{\sqrt{2}}E$. Conversely, strong destructive interference in the S -wave amplitude suppresses its branching fraction, which is slightly smaller than that of the D -wave. It is obvious that $D^0 \rightarrow \omega\rho^0$, dominated by the E amplitude, follows the hierarchy $|S| < |D|$, yielding a larger D -wave branching fraction.

The situation is reversed for the modes $D^0 \rightarrow \omega\bar{K}^{*0}$, $D^0 \rightarrow \omega\omega$, and $D^0 \rightarrow K^{*0}\omega$ characterized by $\frac{1}{\sqrt{2}}(C + E)$ contributions, where the interference pattern is opposite. Specifically, constructive interferences between the C and E amplitudes enhances the S -wave branching fractions, whereas destructive interferences suppresses the D -wave component. These results are consistent with the naive factorization predictions, in which the S -wave component is dominant.

The third category of decay modes involving the E amplitude comprises those governed by $T + E$ amplitudes, including $D^0 \rightarrow K^{*-}\rho^+$, $D^0 \rightarrow \rho^-\rho^+$, $D^0 \rightarrow K^{*-}K^{*+}$, and $D^0 \rightarrow \rho^-K^{*+}$. Here, destructive interference between the T and E amplitudes in the S -wave and constructive interference in the D -wave result in comparable S -wave and D -wave branching fractions. Finally, the remaining decays precessing through T , C or $T + C$ diagrams exhibit a dominant S -wave branching fraction.

As noted in Ref. [17], $D^0 \rightarrow \rho^0\phi$ and $D^0 \rightarrow \omega\phi$ are expected to have identical branching fractions (both total and partial wave) as they share the same C topological amplitude. It is necessary to consider that final state rescattering (e.g., via $D^0 \rightarrow K^{*+}K^{*-}$) can contribute

differently to these two modes [16]. In the FAT approach, the nonfactorization parameters χ_C and ϕ_C , combined with SU(3) breaking effects (specifically, distinct form factors $A^{D^0 \rightarrow \rho}$ and $A^{D^0 \rightarrow \omega}$), effectively incorporate such FSIs. Consequently, the branching fractions predicted by the FAT approach for both $D^0 \rightarrow \rho^0 \phi$ and $D^0 \rightarrow \omega \phi$ are consistent with experimental measurements (Table V). This agreement is particularly notable for the P and D -wave fractions of $D^0 \rightarrow \rho^0 \phi$, which also align with the FSIs predictions of P -wave component Ref. [16]. The partial wave components of $D^0 \rightarrow \omega \phi$, however, await precise measurement by future experiments.

D. Polarization fractions of $D \rightarrow VV$ decays

Based on the fitted parameters in Eq.(16), we calculated the polarization fractions f_L and f_{\parallel} for $D \rightarrow VV$ decays, as listed in Table VIII. The values for f_L and f_{\parallel} , accompanied by their uncertainties summed in quadrature, appear in the table's last two columns, respectively. For clarity in the following discussion, we categorize the 28 decay modes into three groups: those governed exclusively by T , C , or $T + C$ diagrams; those dominated by $T + E$ contributions; and those proceeding through C and E diagrams.

According to Eq.(17), for the first category of decay modes mediated by C or $T + C$ diagrams, their polarization fractions follow the same hierarchy as the nonfactorizable parameters, i.e., $\chi_C^0 > \chi_C^{\parallel}$, which implies $f_L > f_{\parallel}$. In contrast, for modes proceeding only via the T diagram, the longitudinal polarization f_L is comparable to or smaller than f_{\parallel} , as observed in the $D^+ \rightarrow \bar{K}^{*0} K^{*+}$ decay, based on the naive factorization framework.

For the second category of decay modes, where interference occurs between the T and the E amplitudes, their polarization fractions are governed by the strong phase differences between the corresponding helicity amplitudes, $T^{0,\parallel}$ and the $E^{0,\parallel}$. According to Eq.(16), the strong phase difference between the T^0 and E^0 amplitudes is less than $\pi/2$, leading to constructive interference that enhances f_L . Conversely, the strong phase difference between the T^{\parallel} and E^{\parallel} amplitudes exceeds $\pi/2$, resulting in destructive interference that suppresses f_{\parallel} . Consequently, the significant interference between the nonfactorizable E diagram and the T diagram drives the longitudinal polarization f_L to approximately 80%.

Finally, we turn to the third category of modes involving interference between the C and E amplitudes. Given that the strong phase difference satisfy $\phi_E^0 - \phi_C^0 > \pi/2$ while

TABLE VIII: The polarization fractions of $D \rightarrow V_1 V_2$ decays in units of percentage.

Modes	Amplitudes	f_L	f_{\parallel}
$D^0 \rightarrow \rho^0 \phi$	$\frac{1}{\sqrt{2}}C$	48.57 ± 7.25	38.22 ± 7.04
$D^0 \rightarrow \omega \phi$	$\frac{1}{\sqrt{2}}C$	48.58 ± 7.25	38.14 ± 7.04
$D^+ \rightarrow \bar{K}^{*0} \rho^+$	$T + C$	60.68 ± 9.29	36.75 ± 9.23
$D^+ \rightarrow \rho^0 \rho^+$	$-\frac{1}{\sqrt{2}}(T + C)$	64.57 ± 9.59	31.35 ± 9.35
$D^+ \rightarrow \bar{K}^{*0} K^{*+}$	T	39.91 ± 6.18	47.18 ± 6.36
$D^+ \rightarrow \omega \rho^+$	$\frac{1}{\sqrt{2}}(T + C)$	60.08 ± 8.96	33.15 ± 8.47
$D^+ \rightarrow \rho^+ \phi$	C	48.71 ± 7.25	38.07 ± 7.03
$D^+ \rightarrow K^{*0} \rho^+$	C	53.33 ± 7.25	35.13 ± 6.88
$D^+ \rightarrow \rho^0 K^{*+}$	$\frac{1}{\sqrt{2}}T$	40.65 ± 6.02	39.69 ± 5.98
$D^+ \rightarrow \omega K^{*+}$	$\frac{1}{\sqrt{2}}T$	40.65 ± 6.02	39.61 ± 5.98
$D_s^+ \rightarrow \phi \rho^+$	T	47.67 ± 6.42	40.68 ± 6.26
$D_s^+ \rightarrow K^{*+} \bar{K}^{*0}$	C	55.70 ± 7.19	33.28 ± 6.74
$D_s^+ \rightarrow K^{*0} \rho^+$	T	48.67 ± 6.25	34.82 ± 5.78
$D_s^+ \rightarrow K^{*+} \rho^0$	$\frac{1}{\sqrt{2}}C$	61.35 ± 6.92	29.34 ± 6.37
$D_s^+ \rightarrow K^{*+} \omega$	$\frac{1}{\sqrt{2}}C$	60.97 ± 6.95	29.61 ± 6.40
$D_s^+ \rightarrow \phi K^{*+}$	$T + C$	59.79 ± 9.50	36.91 ± 9.42
$D_s^+ \rightarrow K^{*0} K^{*+}$	$T + C$	61.69 ± 9.90	33.83 ± 9.70
$D^0 \rightarrow K^{*-} \rho^+$	$T + E$	84.80 ± 5.76	4.39 ± 4.51
$D^0 \rightarrow \rho^- \rho^+$	$T + E$	83.19 ± 5.22	2.16 ± 2.90
$D^0 \rightarrow K^{*-} K^{*+}$	$T + E$	79.05 ± 7.16	7.35 ± 5.93
$D^0 \rightarrow \rho^- K^{*+}$	$T + E$	77.69 ± 6.33	3.75 ± 3.82
$D^0 \rightarrow \rho^0 \bar{K}^{*0}$	$\frac{1}{\sqrt{2}}(C - E)$	72.23 ± 10.23	12.57 ± 8.88
$D^0 \rightarrow \rho^0 \rho^0$	$\frac{1}{2}(E - C)$	77.43 ± 9.46	10.32 ± 8.13
$D^0 \rightarrow K^{*0} \rho^0$	$\frac{1}{\sqrt{2}}(C - E)$	72.23 ± 10.23	12.57 ± 8.88
$D^0 \rightarrow \omega \bar{K}^{*0}$	$\frac{1}{\sqrt{2}}(C + E)$	41.36 ± 7.98	51.82 ± 7.79
$D^0 \rightarrow \omega \omega$	$\frac{1}{2}(C + E)$	45.43 ± 8.32	48.87 ± 8.06
$D^0 \rightarrow K^{*0} \omega$	$\frac{1}{\sqrt{2}}(C + E)$	41.36 ± 7.98	51.82 ± 7.79
$D^0 \rightarrow \omega \rho^0$	E	38.16 ± 14.21	61.59 ± 14.18

$\phi_E^{\parallel} - \phi_C^{\parallel} < \pi/2$, we observe destructive interference in the longitudinal component and constructive interference in the transverse component for decays with $C + E$ contributions. Consequently, f_L is suppressed while f_{\parallel} is enhanced, yielding $f_{\parallel} > f_L$. This hierarchy also holds for the $D^0 \rightarrow \omega\rho^0$ decay, which is governed exclusively by the E amplitude. In contrast, for modes dominated by $C - E$ interference, f_L is enhanced and f_{\parallel} is suppressed, resulting in a dominant longitudinal polarization of $f_L \sim 70\%$. Notably, our prediction for f_L in the $D^0 \rightarrow \rho^0\rho^0$ decay agree well with the experimental measurement of $(71 \pm 4 \pm 2)\%$ reported by the FOCUS Collaboration [7].

IV. CONCLUSION

Within the FAT framework, we perform a systematical analysis of $D \rightarrow VV$ decays. Four types of topological diagrams, T , C , E , and A , contribute to these decays through weak interactions. The T amplitude is calculated using naive factorization. However, the nonfactorizable C and E amplitudes are described by only two sets of universal parameters, $\chi_C^{0,\parallel,\perp}, \phi_C^{0,\parallel,\perp}$ and $\chi_E^{0,\parallel}, \phi_E^{0,\parallel}$, respectively, for all $D \rightarrow VV$ modes after form factors and decay constants are factored out. This demonstrates that SU(3) breaking effects are naturally incorporated in the FAT approach, which keeps the number of free parameters minimal. Specifically, these parameters characterizing the nonfactorizable contributions of the C and E amplitudes, together with the factorization scale μ of the Wilson coefficient $a_1(\mu)$ for T amplitude, constitute 11 free parameters fitted globally to 36 experimental data points. The obtained nonfactorizable parameters are determined with high precise, except for ϕ_E^{\parallel} .

The fitted parameters yield topological amplitude hierarchies of $|C^0| > |T^0| > |E^0|$ and $|T^{\parallel(\perp)}| \sim |C^{\parallel(\perp)}| > |E^{\parallel(\perp)}|$, indicating that the nonfactorizable C contribution is comparable to the factorizable T contributions. Polarization amplitudes follow $|\mathcal{A}^0| > |\mathcal{A}^{\parallel}| > |\mathcal{A}^{\perp}|$ for the T and C amplitudes, contrary to the naive factorization prediction. Thus, the longitudinal polarization f_L dominates in modes governed by the T or C amplitudes. However, in decays with T and E , or C and E interference, strong phases $\phi_{E,C}^{0,\parallel}$ can possibly resulting in $f_L < f_{\parallel}$. Finally, the partial wave hierarchy $|S| < |D|$ yields a dominant D -wave branching fraction in E diagram mediated decays, contrary to the naive S -wave dominance prediction.

With the fitted nonfactorizable parameters, we predict the branching fractions and polarization fractions for 28 decay modes of $D \rightarrow VV$. Our results are in agreement with the

current experimental data within uncertainties. For modes involving the $C - E$ amplitudes, such as $D^0 \rightarrow \rho^0 \bar{K}^{*0}$, and modes governed by E , like $D^0 \rightarrow \omega \rho^0$, the S -wave branching fractions are slightly smaller than those of the D -wave. This is in contrary to naive factorization estimations but agree with current observations. Regarding polarization fractions, only one data point, f_L of $D^0 \rightarrow \rho^0 \rho^0$, is available for comparison with our theoretical predictions, and they agree well. Predictions for unobserved decay modes await for test by upcoming experimental studies, especially those with branching fractions in order of $10^{-3} - 10^{-2}$, the D -wave dominated modes, and modes exhibiting $f_{\parallel} > f_L$.

Acknowledgments

We are grateful to Chao Wang for useful discussion. The work is supported by the National Natural Science Foundation of China under Grants No.12465017, No.12105148, No.12075126.

-
- [1] **BaBar** Collaboration, B. Aubert et al., *Rates, polarizations, and asymmetries in charmless vector-vector B meson decays*, Phys. Rev. Lett. **91** (2003) 171802, [[hep-ex/0307026](#)].
 - [2] **Belle** Collaboration, K. F. Chen et al., *Measurement of branching fractions and polarization in $B \rightarrow \phi K^{(*)}$ decays*, Phys. Rev. Lett. **91** (2003) 201801, [[hep-ex/0307014](#)].
 - [3] **MARK-III** Collaboration, D. Coffman et al., *Resonant substructure in anti- K π π π decays of D mesons*, Phys. Rev. D **45** (1992) 2196–2211.
 - [4] **BESIII** Collaboration, M. Ablikim et al., *Amplitude analysis of $D^0 \rightarrow K^- \pi^+ \pi^+ \pi^-$* , Phys. Rev. D **95** (2017), no. 7 072010, [[arXiv:1701.08591](#)].
 - [5] **BESIII** Collaboration, M. Ablikim et al., *Amplitude analysis of $D^0 \rightarrow \pi^+ \pi^- \pi^+ \pi^-$ and $\pi^+ \pi^- \pi^0 \pi^0$* , Chin. Phys. C **48** (2024), no. 8 083001, [[arXiv:2312.02524](#)].
 - [6] **BESIII** Collaboration, M. Ablikim et al., *Amplitude analysis and branching fraction measurement of the decay $D_s^+ \rightarrow K^+ \pi^+ \pi^- \pi^0$* , JHEP **09** (2022) 242, [[arXiv:2205.13759](#)].
 - [7] **FOCUS** Collaboration, J. M. Link et al., *Study of the $D^0 \rightarrow \pi^- \pi^+ \pi^- \pi^+$ decay*, Phys. Rev. D **75** (2007) 052003, [[hep-ex/0701001](#)].
 - [8] P. d’Argent, N. Skidmore, J. Benton, J. Dalseno, E. Gersabeck, S. Harnew, P. Naik,

- C. Prouve, and J. Rademacker, *Amplitude Analyses of $D^0 \rightarrow \pi^+\pi^-\pi^+\pi^-$ and $D^0 \rightarrow K^+K^-\pi^+\pi^-$ Decays*, JHEP **05** (2017) 143, [[arXiv:1703.08505](#)].
- [9] A. N. Kamal, R. C. Verma, and N. Sinha, *$D, D_{(s)}^+ \rightarrow VV$ decays in two models: An $SU(3)$ symmetry model and a factorization model with final state interactions*, Phys. Rev. D **43** (1991) 843–854.
- [10] M. Bauer, B. Stech, and M. Wirbel, *Exclusive Nonleptonic Decays of $D, D_{(s)}$, and B Mesons*, Z. Phys. C **34** (1987) 103.
- [11] H.-Y. Cheng and C.-W. Chiang, *Long-Distance Contributions to $D^0 - \bar{D}^0$ Mixing Parameters*, Phys. Rev. D **81** (2010) 114020, [[arXiv:1005.1106](#)].
- [12] T. Uppal and R. C. Verma, *Branching ratios for $D \rightarrow VV$ decays in presence of smearing effects due to rho meson width*, Z. Phys. C **56** (1992) 273–277.
- [13] P. F. Bedaque, A. K. Das, and V. S. Mathur, *Two-body nonleptonic decays of charmed mesons*, Phys. Rev. D **49** (1994) 269–274, [[hep-ph/9307296](#)].
- [14] B. Bajc, S. Fajfer, R. J. Oakes, and S. Prelovsek, *Nonleptonic two-body charmed meson decays in an effective model for their semileptonic decays*, Phys. Rev. D **56** (1997) 7207–7215, [[hep-ph/9706223](#)].
- [15] I. Hinchliffe and T. A. Kaeding, *Nonleptonic two-body decays of D mesons in broken $SU(3)$* , Phys. Rev. D **54** (1996) 914–928, [[hep-ph/9502275](#)].
- [16] Y. Cao, Y. Cheng, and Q. Zhao, *Resolving the polarization puzzles in $D^0 \rightarrow VV$* , Phys. Rev. D **109** (2024), no. 7 073002, [[arXiv:2303.00535](#)].
- [17] H.-Y. Cheng and C.-W. Chiang, *Updated analysis of $D \rightarrow PP, VP$, and VV decays: Implications for $K_S^0 - K_L^0$ asymmetries and $D^0 - \bar{D}^0$ mixing*, Phys. Rev. D **109** (2024), no. 7 073008, [[arXiv:2401.06316](#)].
- [18] H.-Y. Cheng and C.-W. Chiang, *CP violation in quasi-two-body $D \rightarrow VP$ decays and three-body D decays mediated by vector resonances*, Phys. Rev. D **104** (2021), no. 7 073003, [[arXiv:2104.13548](#)].
- [19] Q. Qin, H.-n. Li, C.-D. Lü, and F.-S. Yu, *Branching ratios and direct CP asymmetries in $D \rightarrow PV$ decays*, Phys. Rev. D **89** (2014), no. 5 054006, [[arXiv:1305.7021](#)].
- [20] H. Zheng, J.-R. Dong, and S.-H. Zhou, *Updated branching ratios and CP asymmetries in $D \rightarrow PV$ decays*, Phys. Rev. D **113** (2026), no. 3 036004, [[arXiv:2511.10389](#)].
- [21] J. Wang and Q. Zhao, *Combined analysis of the singly-Cabbibo-suppressed decays of*

- $D^0 \rightarrow VP$, [arXiv:2601.10437].
- [22] H.-Y. Cheng and C.-W. Chiang, *Two-body hadronic charmed meson decays*, Phys. Rev. D **81** (2010) 074021, [arXiv:1001.0987].
- [23] H.-Y. Cheng and C.-W. Chiang, *Direct CP violation in two-body hadronic charmed meson decays*, Phys. Rev. D **85** (2012) 034036, [arXiv:1201.0785]. [Erratum: Phys.Rev.D 85, 079903 (2012)].
- [24] S.-H. Zhou, Y.-B. Wei, Q. Qin, Y. Li, F.-S. Yu, and C.-D. Lu, *Analysis of Two-body Charmed B Meson Decays in Factorization-Assisted Topological-Amplitude Approach*, Phys. Rev. D **92** (2015), no. 9 094016, [arXiv:1509.04060].
- [25] S.-H. Zhou, Q.-A. Zhang, W.-R. Lyu, and C.-D. Lü, *Analysis of Charmless Two-body B decays in Factorization Assisted Topological Amplitude Approach*, Eur. Phys. J. C **77** (2017), no. 2 125, [arXiv:1608.02819].
- [26] H.-n. Li, C.-D. Lu, and F.-S. Yu, *Branching ratios and direct CP asymmetries in $D \rightarrow PP$ decays*, Phys. Rev. D **86** (2012) 036012, [arXiv:1203.3120].
- [27] C. Wang, Q.-A. Zhang, Y. Li, and C.-D. Lu, *Charmless $B_{(s)} \rightarrow VV$ Decays in Factorization-Assisted Topological-Amplitude Approach*, Eur. Phys. J. C **77** (2017), no. 5 333, [arXiv:1701.01300].
- [28] Q. Qin, C. Wang, D. Wang, and S.-H. Zhou, *The factorization-assisted topological-amplitude approach and its applications*, Front. Phys. (Beijing) **18** (2023), no. 6 64602, [arXiv:2111.14472].
- [29] H.-Y. Jiang, F.-S. Yu, Q. Qin, H.-n. Li, and C.-D. Lü, *D^0 - \bar{D}^0 mixing parameter y in the factorization-assisted topological-amplitude approach*, Chin. Phys. C **42** (2018), no. 6 063101, [arXiv:1705.07335].
- [30] D. Wang, F.-S. Yu, P.-F. Guo, and H.-Y. Jiang, *$K_S^0 - K_L^0$ asymmetries in D-meson decays*, Phys. Rev. D **95** (2017), no. 7 073007, [arXiv:1701.07173].
- [31] F.-S. Yu, D. Wang, and H.-n. Li, *CP asymmetries in charm decays into neutral kaons*, Phys. Rev. Lett. **119** (2017), no. 18 181802, [arXiv:1707.09297].
- [32] S.-H. Zhou and C.-D. Lü, *Extraction of the CKM phase γ from the charmless two-body B meson decays*, Chin. Phys. C **44** (2020), no. 6 063101, [arXiv:1910.03160].
- [33] S.-H. Zhou, R.-H. Li, Z.-Y. Wei, and C.-D. Lu, *Analysis of three-body charmed B-meson decays under the factorization-assisted topological-amplitude approach*, Phys. Rev. D **104**

- (2021), no. 11 116012, [[arXiv:2107.11079](#)].
- [34] S.-H. Zhou, X.-X. Hai, R.-H. Li, and C.-D. Lu, *Analysis of three-body charmless B-meson decays under the factorization-assisted topological-amplitude approach*, Phys. Rev. D **107** (2023), no. 11 116023, [[arXiv:2305.02811](#)].
- [35] S.-H. Zhou, R.-H. Li, and X.-Y. Lü, *Analysis of three-body decays $B \rightarrow D(V \rightarrow) PP$ under the factorization-assisted topological-amplitude approach*, Phys. Rev. D **110** (2024), no. 5 056001, [[arXiv:2406.00373](#)].
- [36] J. Ou-Yang, R.-H. Li, and S.-H. Zhou, *Analysis of three-body charmed B meson decays $B \rightarrow D(V^* \rightarrow) VP$* , Phys. Rev. D **112** (2025), no. 5 056005, [[arXiv:2506.14675](#)].
- [37] X.-D. Zhou and S.-H. Zhou, *Analysis of three-body hadronic D-meson decays*, Phys. Rev. D **111** (2025), no. 11 116008, [[arXiv:2503.18593](#)].
- [38] W.-F. Wang, J.-Y. Xu, S.-H. Zhou, and P.-P. Shi, *Contributions of $\rho(770, 1450) \rightarrow \omega\pi$ for the Cabibbo-favored $D \rightarrow h\omega\pi$ decays*, [[arXiv:2502.11159](#)].
- [39] M. Wirbel, B. Stech, and M. Bauer, *Exclusive Semileptonic Decays of Heavy Mesons*, Z. Phys. C **29** (1985) 637.
- [40] **Particle Data Group** Collaboration, S. Navas et al., *Review of particle physics*, Phys. Rev. D **110** (2024), no. 3 030001.
- [41] R. C. Verma, *Decay constants and form factors of s-wave and p-wave mesons in the covariant light-front quark model*, J. Phys. G **39** (2012) 025005, [[arXiv:1103.2973](#)].
- [42] H.-Y. Cheng, C.-K. Chua, and C.-W. Hwang, *Covariant light front approach for s wave and p wave mesons: Its application to decay constants and form-factors*, Phys. Rev. D **69** (2004) 074025, [[hep-ph/0310359](#)].
- [43] P. Ball, G. W. Jones, and R. Zwicky, *$B \rightarrow V\gamma$ beyond QCD factorisation*, Phys. Rev. D **75** (2007) 054004, [[hep-ph/0612081](#)].
- [44] A. Bharucha, D. M. Straub, and R. Zwicky, *$B \rightarrow V\ell^+\ell^-$ in the Standard Model from light-cone sum rules*, JHEP **08** (2016) 098, [[arXiv:1503.05534](#)].
- [45] P. Gelhausen, A. Khodjamirian, A. A. Pivovarov, and D. Rosenthal, *Decay constants of heavy-light vector mesons from QCD sum rules*, Phys. Rev. D **88** (2013) 014015, [[arXiv:1305.5432](#)]. [Erratum: Phys.Rev.D 89, 099901 (2014), Erratum: Phys.Rev.D 91, 099901 (2015)].
- [46] **BESIII** Collaboration, M. Ablikim et al., *Amplitude analysis and branching-fraction*

- measurement of $D_s^+ \rightarrow K_S^0 K^- \pi^+ \pi^+$, Phys. Rev. D **103** (2021), no. 9 092006, [arXiv:2102.03808].
- [47] **BESIII** Collaboration, M. Ablikim et al., *Amplitude analysis and branching fraction measurement of $D_s^+ \rightarrow K^- K^+ \pi^+ \pi^0$* , Phys. Rev. D **104** (2021), no. 3 032011, [arXiv:2103.02482].
- [48] **BESIII** Collaboration, M. Ablikim et al., *First Measurement of Polarizations in the Decay $D^0 \rightarrow \omega \phi$* , Phys. Rev. Lett. **128** (2022), no. 1 011803, [arXiv:2108.02405].
- [49] **BESIII** Collaboration, M. Ablikim et al., *Amplitude analysis and branching fraction measurement of the decay $D^+ \rightarrow K_S^0 \pi^+ \pi^0 \pi^0$* , JHEP **09** (2023) 077, [arXiv:2305.15879].
- [50] **LHCb** Collaboration, R. Aaij et al., *Studies of the resonance structure in $D^0 \rightarrow K^\mp \pi^\pm \pi^\pm \pi^\mp$ decays*, Eur. Phys. J. C **78** (2018), no. 6 443, [arXiv:1712.08609].
- [51] **LHCb** Collaboration, R. Aaij et al., *Search for CP violation through an amplitude analysis of $D^0 \rightarrow K^+ K^- \pi^+ \pi^-$ decays*, JHEP **02** (2019) 126, [arXiv:1811.08304].